

ELSA: Partial Weight Freezing for Overhead-Free Sparse Network Deployment

Paniz Halvachi
Sharif University of Technology

Alexandra Peste

Dan Alistarh
Institute of Science and Technology Austria (ISTA)

Christoph H. Lampert

Abstract

We present *ELSA*, a practical solution for creating deep networks that can easily be deployed at different levels of sparsity. The core idea is to embed one or more sparse networks within a single dense network as a proper subset of the weights. At prediction time, any sparse model can be extracted effortlessly simply by zeroing out weights according to a predefined mask. *ELSA* is simple, powerful and highly flexible. It can use essentially any existing technique for network sparsification and network training. In particular, it does not restrict the loss function, architecture or the optimization technique. Our experiments show that *ELSA*'s advantages of flexible deployment comes with no or just a negligible reduction in prediction quality compared to the standard way of using multiple sparse networks that are trained and stored independently.

1. Introduction

Deep learning has revolutionized a myriad of domains, but the high computational and memory cost of large models remains a hurdle. Network sparsification techniques have been explored to mitigate these issues. However, most existing approaches focus only on creating individual sparse models with as-good-as-possible accuracy-vs-sparsity trade-off, but they do not consider the ease of their practical deployment.

As an illustrative example, consider the situation of a smartphone app that runs a deep network for object detection. Depending on the phone hardware, networks of different sizes should be used to ensure real-time capabilities. Traditionally, there are two ways to achieve this: either, the app binary already contains all possible networks and it chooses an appropriate one at execution time. This is efficient and easy in deployment, but it has the disadvantage of an excessively large initial download. The app size will grow linearly with the number of possible networks, even though only a single one will actually be used in the end. Alternatively, the app binary would not contain the weights for any network. Instead, it decides on a suitable network size when it is started for the first time, and down-

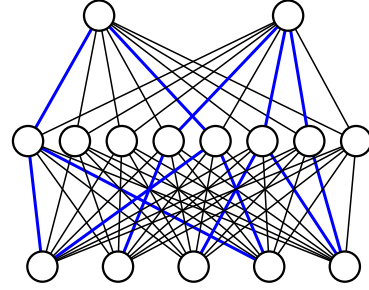


Figure 1. Illustration of an ELSA-Net: the weights of a trained sparse network (blue) are embedded as a proper subset within the weights of a dense network. At prediction time, the complete dense network can be run as is, or the sparse network can be extracted effortlessly by setting all other (non-blue) weights to 0. The extracted sparse network is identical to the one originally embedded, allowing for state-of-the-art accuracy without the need for fine-tuning or other adjustments.

loads the weights for this network from an online resource. This, however, leads to a worse user experience. The first start of the app will incur a long latency and unexpected large data transmission. It might also trigger security concerns if an app downloads large files from an external server. More effective than the above two cases, would be a setup in which the app binary contains just one network, from which smaller and more efficient models could be constructed on-the-fly to match the device hardware. In the context of network sparsification, this task is known as *one-shot pruning*.

In this work, we introduce *ELSA (Efficient Layer Sparsification Approach)*, a technique that allows one-shot pruning of deep networks at deployment time to a degree not achieved before. *ELSA* is, in fact, not a new network sparsification technique, but a new way of constructing, storing, and retrieving sparse networks, where the individual networks are produced using any existing technique for network sparsification. The core idea is illustrated in Figure 1: the weights of a trained sparse network (blue) are embedded as a proper subset within the weights of a dense network. At prediction time, the complete dense network

can be run as is, or the sparse network can be extracted effortlessly by setting all other (non-blue) weights to 0. The extracted sparse network is identical to the one originally embedded, allowing for state-of-the-art accuracy without the need for fine-tuning or other adjustments.

By iterating the above procedure, it is also possible to embed multiple models, of different sparsity levels, within a single dense one, thereby providing a choice between different sparsity levels at prediction time.

Networks produced by ELSA (ELSA-Nets) can have arbitrary architectures, and they can be trained, evaluated, and deployed using standard techniques with at most minor adjustments. At prediction time, they can be used either in dense or in sparse form with negligible overhead.

2. Method

In this section we first introduce the ELSA-method of storing a sparse network within a dense one. We then discuss a multi-level extension that allows creating and storing multiple networks of different sparsity levels still within a single dense network.

2.1. ELSA

At the core of ELSA lies the observation that the weights of a sparse networks can be embedded inside a dense one, and later recovered without loss of quality. While previously proposed to prevent catastrophic forgetting in continual multi-task learning [24, 34], we instantiate the idea in the context of one-shot network pruning.

Its working principle is illustrated in Figure 2 (a)–(c). The starting point is an ordinary dense network (a), typically pretrained to high accuracy. To this, one applies an arbitrary *sparsification* method, resulting in a sparse network (b). Now, the subset of weights that belong to the sparse network are *frozen* (illustrated in blue). This means that their values will be prevented from changing in subsequent steps. Then, a *densification* step is performed. This trains the non-frozen weights (which previously all had value 0), thereby again ending up with a dense network (c).

A brief analysis shows the rationality of the process: because the choice of sparsification method is discretionary, the sparse network can be of state-of-the-art quality. The dense network contains the sparse one as a fixed subset, but it has additional learning capacity. As such, one can expect the resulting dense network to be of higher accuracy than the sparse one, ideally recovering or even exceeding the accuracy of the initial dense network.

The sparse network can be extracted effortlessly from the dense one, simply by setting a predefined set of network weights to zero. The resulting sparse network is identical to the originally trained one, so its efficiency and quality are known a priori, and no further finetuning or other

Algorithm 1 ELSA

input network with weights $\theta \in \mathbb{R}^D$
input target sparsity level α
input (optional) frozen/learnable mask $M \in \{0, 1\}^D$
1: **if** no M provided **then** $M \leftarrow \mathbf{1} \in \mathbb{R}^D$
2: $\theta_{\text{sparse}} \leftarrow \text{sparsify}(\theta, M, \alpha)$
3: $M \leftarrow M \odot \mathbb{1}(\theta \neq 0)$ /* freeze non-zero weights */
4: $\theta_{\text{dense}} \leftarrow \text{densify}(\theta_{\text{sparse}}, M)$
output θ_{dense}, M

adjustments are needed to give it high accuracy. The latter aspect is the main difference to prior one-shot pruning works: these are also able to create sparse networks, but cannot guarantee their quality. Typically, they also require some additional processing and data to achieve satisfying accuracy (see our discussion in Section 4).

Algorithm 1 provides pseudo-code for the procedure described above. Whether any network weight is *frozen* (0) or *learnable* (1) is indicated by a binary mask, M . For consistency with later extensions we allow an initial mask as optional input to the algorithm. For single-stage ELSA, where no weights are frozen initially, we initialize the mask as a vector of all 1s (line 1). The *sparsify* step (line 2) now calls an arbitrary subroutine for network sparsification. In the case a non-trivial mask was provided, the sparsification method must respect the mask, i.e. it may not change or remove weights indicated as frozen. This is hardly a restriction, though, as we will discuss below. After the sparsification, the mask is updated to mark all weights in the sparse subnetwork, i.e. all non-zero ones, as frozen (line 3). Here, \odot indicates componentwise multiplication, and $\mathbb{1}(P) = 1$ if a predicate, P , is true and $\mathbb{1}(P) = 0$ otherwise, also applied componentwise in our setting. The other weights remain learnable.

The subsequent *densify* step can again an arbitrary subroutine for network training, as long as it respects the mask, i.e. does not change frozen weights (line 4). Finally, the algorithm outputs the weights of the dense network, θ_{dense} , together with the updated binary mask, M .

At prediction time, the sparse network can be extracted effortlessly from the dense one as $\theta_{\text{sparse}} = (\mathbf{1} - M) \odot \theta_{\text{dense}}$. Because all its weights were frozen after the sparsification step and did not change during the subsequent densification, it is identical to the originally embedded one.

2.2. Multi-level ELSA

Algorithm 1 takes as input a dense network and a binary mask, and it outputs again a dense network and a binary mask. As such, it is clear that the algorithm can also be run iteratively. Figure 2 (c)–(e) illustrates a second invocation of ELSA at a lower sparsity level: the input now is a dense network with some frozen (blue) weights (c). *sparsify*

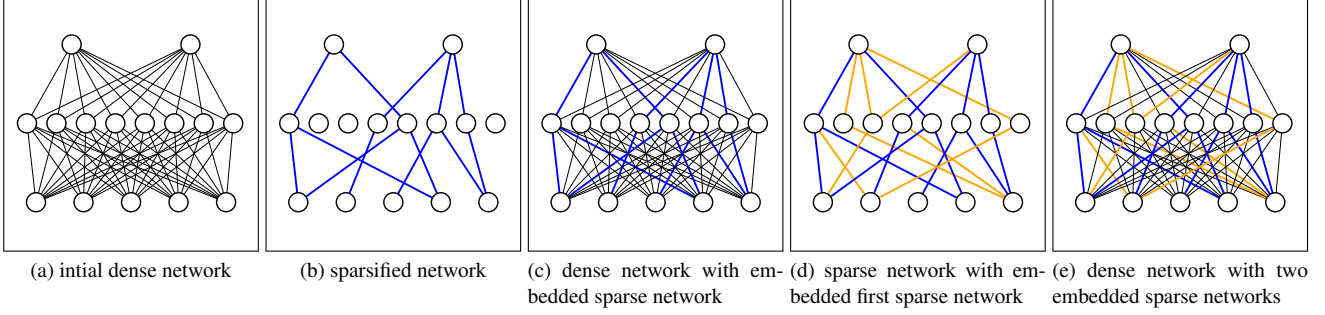


Figure 2. Illustration of *ELSA* (a)–(c) and *multi-level ELSA* (a)–(e).

Algorithm 2 Multi-level ELSA

input network with weights $\theta^{(0)} \in \mathbb{R}^D$
input target sparsity levels $\alpha^{(1)} > \alpha^{(2)} > \dots > \alpha^{(T)}$
1: $M^{(0)} \leftarrow \mathbf{1} \in \mathbb{R}^D$, $N^{(0)} \leftarrow \mathbf{1} \in \mathbb{R}^D$
2: **for** $t = 1, \dots, T$ **do**
3: $\theta^{(t)}, M^{(t)} \leftarrow \text{ELSA}(\theta^{(t-1)}, M^{(t-1)}, \alpha^{(t)})$
4: $N^{(t)} \leftarrow N^{(t-1)} + M^{(t)}$
5: **end for**
output $\theta^{(T)}, N^{(T)}$

produces a sparse network that contains all originally frozen weights as well as some additional ones (orange). These are then frozen, too (d). *densify* again produces a dense network from this that now contains two embedded sparse networks (e).

Algorithm 2 provides pseudo-code for multi-level ELSA for any number of steps and any decreasing sequence of sparsity levels. After initializing the mask (line 1), it repeatedly calls ELSA. The output of each call serves as input for the next one (line 3). Over T rounds, it computes an alternating sequence of *sparse and dense models*, $\theta_{\text{sparse}}^{(1)}, \theta_{\text{dense}}^{(1)}, \theta_{\text{sparse}}^{(2)}, \dots, \theta_{\text{sparse}}^{(T)}, \theta_{\text{dense}}^{(T)}$, and well as a sequence of *binary masks*, $M^{(1)}, \dots, M^{(T)}$, and *aggregate counters*, $N^{(1)}, \dots, N^{(T)}$. Note that the index (t) in Algorithm 2 is just a notational convention. Really, none of the intermediate quantities, θ , M or N , need to be memorized, but they can simply be overwritten with their updated counterpart. Consequently, the memory usage is constant, regardless of T , and the overhead compared to ordinary network training is small.

The use of ELSA as a subroutine means that each sparse network could be recovered from the subsequent dense network. For this, one sets all weights to zero that are not part of the subnetwork, i.e. one multiplies the dense model’s weights with the associate binary sparsity mask, $\theta_{\text{sparse}}^{(t)} = (\mathbf{1} - M^{(t)}) \odot \theta_{\text{dense}}^{(t)}$. By construction, all weights corresponding to zero entries of $M^{(t)}$ will be frozen in subsequent steps and therefore remain unchanged until the

end of the algorithm. Consequently, the same sparse network can also be extracted from the final dense model as $\theta_{\text{sparse}}^{(t)} = (\mathbf{1} - M^{(t)}) \odot \theta_{\text{dense}}^{(T)}$.

Preserving all intermediate masks is not required, either: by construction they have a nested structure, such that once a mask entry is 0, it will also be 0 in all later masks. Consequently, it suffices to store at which time step (if any) a weight was frozen for the first time, i.e. the value t for which it first received a 0 entry in the mask. This is the role of the counters $N^{(t)}$, which in each step are incremented only for those weights that are not frozen (line 4). After T steps, binary masks for each sparsity level, α_t , can be extracted from the final counters $N^{(T)}$ as $M^{(t)} = \mathbf{1} - \mathbb{1}(N^{(T)} \leq t)$. Weights with counter value $T + 1$ are not part of any sparse networks but only contribute to the final dense one. Ultimately, all sparse networks are available as

$$\theta_{\text{sparse}}^{(t)} = \mathbb{1}(N^{(T)} \leq t) \odot \theta_{\text{dense}}^{(T)}. \quad (1)$$

in identical form to when they were constructed.

Overall, multi-level ELSA extends single-level ELSA to allow one-shot pruning of a single dense network to different sparsity levels. At the same time it preserves the desirable property that the extracted networks are bit-exact identical to the ones stored at training time. They are ready-to-use and their performance is known a priori.

2.3. Choice of Subroutines

ELSA’s central components are the subroutines *sparsify* and *densify*. The choice of densification routine is fully flexible, as its task is only to improve the accuracy of a given sparse network by learning values for the initially zero-valued weights without changing the initially non-zero ones. Consequently, any standard network training method can be used, as long as it allows restricting the set of weights that are allowed to change [3, 31, 33]. In particular, this is the case for standard iterative optimizers, such as SGD [30] or Adam [19]: all one has to do is multiply the computed updates by the current mask before adding them to the weights. In some

case, the densification can even be skipped at intermediate stages. One example of this is if the sparsification routine operates via an implicit densification step anyway, as will be the case in some of our experiments.

The sparsification routine can also be chosen freely, as long as it supports partially sparsifying a network in a way such that a given subset of weights must not change. The latter property holds in particular for most score-based methods. For example, assume *top-K* magnitude pruning [13]. For each entry, θ_i , of the network weights one computes an *importance score*, s_i , for example, the weight’s absolute value [16] or its entry in the loss gradient [18, 29]. One then keeps the K weights with largest scores and sets the others to 0. This process has a straight-forward extension to the situation in which some weights are frozen: setting $s_i = \infty$ (or any large enough finite value) for all frozen weights, they will fall automatically into the top- K set and thereby avoid being removed. Note that this scenario applies not only to *unstructured* sparsity, but also to *semi-structured* or *structured sparsity*, with the scores defined on the right level of granularity [22, 38].

2.4. Extension: Overhead-Free ELSA

Besides the dense network, Algorithm 2 produces the counter structure, $N^{(t)}$, which stores which subset of network weights should be used at which level of sparsity. Storing the counter requires $\tau := \lceil \log_2(T + 1) \rceil$ bits per weight entry. In practice, however, we can save ourselves even this overhead, and dispense with the counter structure completely. For this we observe that for compatibility reasons it is common practice to store and distribute network weights as 32-bit floating point numbers, even if the least significant bits of these values have no effect on the network computation, and—at least on GPUs—the actual computations happens at a lower precision anyway.¹

Consequently, we can store the counter values directly as part of the network weights: after each sparsification step, t , we overwrite the least significant τ bits of the newly found non-zero weights with the binary representation of the value t . We do not change weights that were frozen in previous steps (their least significant bits already contain their respective time step), and zero-valued weights, i.e. weights that are not part of the sparse network, are not influenced either. In storing the final dense network, we set its least significant bits to 0, thereby uniquely marking them as not part of any sparse subset.

At deployment time, all that is required to extract a sub-network of desired sparsity level, α_t , is to load the dense

network and keep only those weights with least significant bits $\{1, \dots, t\}$, while setting the others to 0:

$$\theta_{\text{sparse}}^{(t)} = \mathbb{1}(0 < \text{lsb}_\tau(\theta^{(T)}) \leq t) \odot \theta_{\text{dense}}^{(T)}, \quad (2)$$

where the function lsb_τ returns the integer represented by the τ least significant bits of the argument (interpreted as just a sequence of bits). Equation (2) can easily be implemented using bit masking.

Subsequently, for every practical number of sparsity levels, storage requirements for a full ELSA-net is identical to that of a single dense network, and the computational overhead for extracting any desired subnetwork is negligible. The format even allows *streaming* extraction, because the decision if a weight should be included or not can be made immediately after reading its value. Consequently, the dense model never even has to be stored fully on the client device.

2.5. Extension: Batchnorm Statistics

Both variants of ELSA can be applied out-of-the-box for networks consisting of arbitrary layers with learnable weights, let them be fully-connected, convolutional or attention-based. However, a different situation emerges for *batch normalization* layers. These have not only learnable weights, but also a separate set of *batchnorm statistics*, which are determined at training time but used only at prediction time. Those, typically a *mean* and a *variance* vector, cannot be pruned and must be adapted to the activation values of the preceding network layer. As a consequence, the optimal batchnorm statistics will differ between different sparse networks.

There is a number of possibilities how to add this issue. Most straight-forward is to simply store the batchnorm statistics for each sparsity level and look them up at deployment time. In contrast to the discussion above, this imposes only a minor overhead, because the batchnorm statistics are typically several orders of magnitude smaller than the set of network weights.

In a setting of a likely domain shift, suitable batchnorm statistics can be computed at prediction time from a subset of the prediction time data. This is possible because the batchnorm statistics depend only on the network activations, not on the loss value, so they can be computed also from unlabeled data.

Finally, in some cases it is possible to remove the batch normalization layers all-together from the network by *folding* them into the regular network weights. This option depends on the chosen architecture though, so we do not study it further in this work.

3. Experiments

We report on experiments in two standard setups (ResNet50 on ImageNet, WideResNet-28-10 on CIFAR100) to demon-

¹Trivially so when using low-precision data types, such as `float16` or `bfloat16`, but also when using seemingly full-precision `float32`, because on recent GPUs matrix multiplications are executed by default in an internal `TensorFloat32` representations, which uses only a 10-bit mantissa rather than the 23-bit of the IEEE standard [7].

Table 1. Accuracy of ELSA on CIFAR100 (WideResNet-28-10). Models in the caption *ELSA sparse* are extracted from the *ELSA dense* model by means of Equation 2.

(a) global sparsity			
sparsity level	initial dense	ELSA sparse	ELSA dense
80 (79.9%)	82.2 \pm 0.2	81.3 \pm 0.2	82.2 \pm 0.2
90 (89.9%)	82.2 \pm 0.1	80.8 \pm 0.2	82.1 \pm 0.3
95 (94.9%)	82.3 \pm 0.3	80.1 \pm 0.1	82.2 \pm 0.1
(b) uniform sparsity			
sparsity level	initial dense	ELSA sparse	ELSA dense
80 (79.8%)	82.3 \pm 0.2	81.8 \pm 0.3	82.4 \pm 0.2
90 (89.9%)	82.2 \pm 0.3	81.5 \pm 0.2	82.3 \pm 0.1
95 (94.9%)	82.1 \pm 0.2	80.7 \pm 0.1	82.5 \pm 0.1
(c) N:M sparsity			
sparsity level	initial dense	ELSA sparse	ELSA dense
2:4 (49.9%)	82.1 \pm 0.1	81.7 \pm 0.2	82.3 \pm 0.3
1:4 (74.8%)	82.0 \pm 0.1	81.4 \pm 0.0	82.2 \pm 0.3
1:8 (87.3%)	82.2 \pm 0.1	80.6 \pm 0.2	82.1 \pm 0.2

strates that ELSA works well for relevant model and dataset sizes. We also perform stress test experiments on CIFAR10 that aim at pushing ELSA to its limits.

In all cases, the focus of our experiments is to show that the quality of ELSA-Nets is comparable to that of sparse networks which were trained individually. This fact establishes that it is possible to benefit from the advantages of having a single dense network for deployment while suffering no or almost no loss of accuracy.

Implementation Our implementation of ELSA is written in *jax* [4] based on the *flax* [15] and *jaxpruner* [21] libraries. The source code is provided as supplemental material and will be made public after publication.

Sparsity types and levels Our experiments cover unstructured (*global sparsity* and *uniform (per-layer) sparsity*), as well as semi-structured *N:M sparsity* [7].

Training We train all initial models with standard mini-batch SGD with momentum and Nesterov acceleration. Further details, including hyperparameter choices are provided in the supplementary material.

As exemplary *sparsify* method, we use *gradual magnitude pruning (GMP)* [12], which has proven to be a strong allrounder method that is often on par with more complex techniques [17]. To ensure that no frozen weights are removed during sparsification we change *jaxpruner*’s score computation to yield fixed large values for all frozen weights. As *densify* routine, we use the same procedure as for initial training, just with 100 times lower learning rate. We ensure that frozen weights stay at their given value by multiply the weight updates by the binary mask of which

Table 2. Accuracy of ELSA on ImageNet (ResNet-50). Models in the caption *ELSA sparse* are extracted from the *ELSA dense* model by means of Equation 2.

(a) global sparsity			
sparsity level	initial dense	ELSA sparse	ELSA dense
70 (69.9%)	76.4 \pm 0.1	75.9 \pm 0.1	75.8 \pm 0.2
80 (79.8%)	76.4 \pm 0.0	75.8 \pm 0.1	76.2 \pm 0.1
90 (89.8%)	76.4 \pm 0.0	75.1 \pm 0.1	76.5 \pm 0.1
(b) uniform sparsity			
sparsity level	initial dense	ELSA sparse	ELSA dense
70 (64.3%)	76.4 \pm 0.0	75.9 \pm 0.1	76.0 \pm 0.1
80 (73.5%)	76.4 \pm 0.0	75.7 \pm 0.1	76.1 \pm 0.1
90 (82.7%)	76.4 \pm 0.0	74.3 \pm 0.1	76.1 \pm 0.1
(c) N:M sparsity			
sparsity level	initial dense	ELSA sparse	ELSA dense
2:4 (45.9%)	76.5 \pm 0.1	76.0 \pm 0.1	75.9 \pm 0.1
1:4 (68.9%)	76.5 \pm 0.1	75.1 \pm 0.1	76.2 \pm 0.2
1:8 (80.4%)	76.5 \pm 0.1	72.6 \pm 0.1	76.1 \pm 0.1

weights are learnable.

Internally, GMP works by incrementally increasing the sparsity over its run following a polynomial schedule [2]. As such, it has initial densification implicitly built in, allowing us to dispense with the explicit densification step for the cases of unstructured pruning on ImageNet and CIFAR100.

Comparison to published works As mentioned above, ELSA is not actually a new technique for network sparsification, and we do not claim that it improves the sparsity-accuracy trade-off. Rather, essentially any existing or future technique for network sparsification can be integrated seamlessly into ELSA as its *sparsify* routine. Consequently, the experimental results we report for ELSA should not be seen as attempts to *improving over a baseline*, but rather as evidence that ELSA offers previously unseen functionality reliably across many relevant and state-of-the-art scenarios.

To show that our experiments indeed reflect this setting, we provide reference results from the literature in this section. On the one hand, the accuracy of our initial networks indeed matches what has been reported previously in the literature for vanilla training (standard data augmentation, standard cross-entropy objective): approximately 76% for a ResNet50 on ImageNet2012 [26, 35], above 80% for a WideResNet-28-10 on CIFAR100 [37], and approximately 94% for a SpeedyResNet on CIFAR-10 [1]. On the other hand, the quality of the sparse networks we obtain is also consistent with the literature: sparsifying ResNet50 on ImageNet with GMP to a sparsity level of 90% results in an accuracy loss of 1-2%. For 80% it is below 1%, and for 70% the loss is less than 0.5%, if any [11]. For WideResNet-28-10, similar results hold [27].

3.1. Results

In our experimental results we always report the mean and standard deviation of the models’ accuracy for runs with four random seeds. The sparsity levels in the results tables indicate the chosen sparsity levels for the pruned weights. The actual percentage of zero weights is provided in bracket behind it. This can be smaller, because some layers are excluded from sparsification.

Single-level ELSA We first report on results for the standard ELSA (Algorithm 1), in which a sparse network is embedded transparently within a dense one. Here, by construction and as a defining feature of ELSA, the quality of the embedded sparse network is identical to the one produced by the chosen sparsification technique, because they have identical weights. Our evaluation therefore concentrates the quality of the dense network that ELSA produces by densifying the networks after freezing sparse subnetwork.

Tables 1 and 2 show the results for the different sparsity types and sparsity levels. One can see that, apart from some fluctuations due to randomness in the learning process, the dense models produced by ELSA generally matches the accuracy of the initial model within less than half a percent. Consequently, the advantage of ELSA-Nets, that one can also extract a sparse network from it at prediction time, comes with essentially no drawbacks.

Multi-level ELSA We now report on results for the multi-level ELSA (Algorithm 2), in which multiple sparse networks are embedded within a single dense one. This scenario best matches our motivating example of deploying a network in resource-constrained situations, where one wants to be able to adapt the model sparsity to the target device. As such, our emphasis here lies on the assessing the quality of the sparse networks, in particular the ones created at later stages, when some of the network weights had already previously been frozen.

Tables 3 and 4 show the results. For each sparsity type three networks of different sparsity levels are embedded in a single dense one. In each case we compare the accuracy of the resulting sparse networks to their respective references. For the sparse networks, this is the result of running sparsification independently for each level, i.e. without any weights frozen previously. For the dense output network, the reference is the quality of simply training networks from scratch, as represented by the initial networks that serve as input for ELSA.

One can see that in all cases multi-level ELSA achieves sparse networks of quality comparable with the references. This once again shows that ELSA’s advantage of having all networks embedded in a single parameter set comes without major drawbacks. On CIFAR100, the quality of the ultimate dense network fully matches that of the initial dense

model which was trained from scratch. For ImageNet, the final dense accuracy is in some cases about 0.5%-1% lower than the initial one. One explanation for this fact is that after the last sparsification step a non-negligible subset of weights remains frozen and cannot be changed during densification, thus resulting in a harder optimization problem. On the other hand, this was also the case in our experiments for single-level ELSA for with low sparsity, but there the difference was smaller. Instead, the effect might also just be an artifact of the fact that we use common default hyperparameters for all densification steps, despite the fact that the presence of different rather high-accuracy frozen subnetworks can be expected to change the loss landscape. If the latter is indeed the case, we expect that a more thorough hyperparameter search will increase the results further.

Stress test Finally, we report on a *stress test* experiments that is meant to explore the scalability of multi-level ELSA to a very large number of embedded network. For this, we embed 50 sparse networks within a single dense one. To avoid excessive computational demands we use the SpeedyResNet architecture [1] on the CIFAR10 dataset here. The sparsity levels range from 99% to 50%, corresponding to networks with approximately 50.000 to 2.4 millions non-zero weights out of the original 4.7 million.

Figure 3 illustrates the results: one can see that despite the large number of sparsity levels ELSA’s performance did not degenerate. As it should be, the embedded sparse networks achieve (up to random fluctuations) increasing accuracy with decreasing sparsity. For sparsity levels below a certain threshold (approximately 95% for global sparsity, approximately 90% for uniform sparsity), the accuracy of the sparse models matches or even exceeds the one of the initial dense model, as does the quality of the final dense model produced by ELSA. Note that this effect allows for an intuitive explanation, by observing that the final model has undergone many more training epochs than the initial one. Nevertheless, we find it a noteworthy finding, because it demonstrates that it is possible for the advantage of deploying variable-sparsity ELSA-Nets not only to come without loss of prediction quality, but even with a gain.

4. Related Work

To our knowledge, ELSA is the first method that allows extracting multiple fully trained sparse networks at deployment time from a single dense network. Consequently, there is no direct prior work in the literature with which we could compare quantitatively. There are, however, a number of existing methods that either perform similar steps for different purposes, or that aim for related goals. In this section we discuss how ELSA relates to some of these.

One-shot pruning *One-shot pruning* refers to the task of creating sparse models from dense ones in a single step, i.e.,

Table 3. Accuracy of multi-level ELSA on CIFAR100. All models in the *multi-level ELSA* column are extracted from the same single dense network by means of Equation (2). Models in the *reference* column are the results of sparsifying independently for each level.

(a) global sparsity		
sparsity level	multi-level ELSA	reference
95 (94.9%)	80.1 ± 0.2	80.1 ± 0.1
90 (89.9%)	81.2 ± 0.1	80.8 ± 0.2
80 (79.9%)	81.4 ± 0.1	81.3 ± 0.2
dense	82.1 ± 0.2	82.1 ± 0.1
(b) uniform sparsity		
sparsity level	multi-level ELSA	reference
95 (94.8%)	80.7 ± 0.3	80.7 ± 0.1
90 (89.8%)	81.5 ± 0.1	81.5 ± 0.2
80 (79.8%)	81.8 ± 0.2	81.8 ± 0.3
dense	82.2 ± 0.1	82.2 ± 0.2
(c) N:M sparsity		
sparsity level	multi-level ELSA	reference
1 : 8 (87.3%)	80.6 ± 0.1	80.6 ± 0.2
1 : 4 (74.8%)	81.4 ± 0.2	81.4 ± 0.0
2 : 4 (49.9%)	81.7 ± 0.2	81.7 ± 0.2
dense	82.2 ± 0.2	82.1 ± 0.2

Table 4. Accuracy of multi-level ELSA on ImageNet. All models in the *multi-level ELSA* column are extracted from the same single dense network by means of Equation (2). Models in the *reference* column are the results of sparsifying independently for each level.

(a) global sparsity		
sparsity level	ELSA	reference
90 (89.8%)	75.3 ± 0.0	75.1 ± 0.1
80 (79.8%)	75.9 ± 0.1	75.8 ± 0.1
70 (69.9%)	75.9 ± 0.1	75.9 ± 0.1
dense	76.0 ± 0.2	76.4 ± 0.1
(b) uniform sparsity		
sparsity level	ELSA	reference
90 (82.7%)	74.2 ± 0.1	74.3 ± 0.1
80 (73.5%)	75.4 ± 0.1	75.7 ± 0.1
70 (64.3%)	75.6 ± 0.1	75.9 ± 0.1
dense	75.8 ± 0.1	76.4 ± 0.0
(c) N:M sparsity		
sparsity level	ELSA	reference
1 : 8 (80.4%)	72.6 ± 0.2	72.6 ± 0.1
1 : 4 (68.9%)	74.5 ± 0.1	75.1 ± 0.1
2 : 4 (45.9%)	75.3 ± 0.1	76.0 ± 0.1
dense	75.7 ± 0.1	76.5 ± 0.0

without further fine-tuning or other iterative procedures.

For unstructured sparsity, the state of the art is *CrAM* [28] and its variants. It proposes a specific loss function, inspired by SAM [9], that encourages weight values that result in networks of high accuracy even when top-K pruned. By a special optimization procedure it can be optimized approximately. A shortcoming of *CrAM* is that the sparse networks it produces are trained only implicitly, so their actual quality is not known a priori. *CrAM* also cannot construct batchnorm statistics for them. Instead, these have to be created at prediction time, e.g. from test data.

The empirical results reported by *CrAM* resemble ours: 75.8% and 74.7% accuracy for a ResNet50 trained on ImageNet at 80% and 90% sparsity, respectively. These numbers cannot be directly compared to ELSA, though, because *CrAM* uses a stronger (SAM-like [20]) training objective and tunes the batchnorm statistics at prediction time.²

Other recent works include *SFW-pruning* [25] and *compression-aware SFW* [39]. Both use Frank-Wolfe optimization to learn networks whose weights lie in the convex hull of sparse basis vectors, and should therefore be easier approximateable in a sparse way. Empirically, however, the approaches achieved a worse sparsity-accuracy tradeoff than, for example, *CrAM*, and their performance was not

demonstrated on challenging datasets, such as ImageNet.

For structured sparsity, OTO [6] partitions the weights of a network into specific groups. It identifies which groups do not contribute to the network output and removes those. As such, OTO is less flexible than, e.g., score-based methods, and its effectiveness depends on the underlying architecture. In particular, only modest sparsity levels were reported for standard ResNets.

The OFA [5] approach is very broad in the type of structures that can be varied, including model depth, layer width, kernel size, and input resolution. At training time it learns a large model that encompasses all of these aspect. At prediction time, a step of neural architecture search is performed to find the best substructure for the current setting. A downside of OFA is that it requires the interaction of several non-standard components, which results in a complex training and deployment process.

ELSA differs fundamentally from all of the above methods: due to its modular structure it is highly versatile and not restricted to a specific loss function (such as *CrAM*), optimization technique (as OFA and the SFW methods) or network architectures (such as OTO). Also, all the above methods train with via proxy tasks. The actual sparse networks are created for the first time at prediction time. ELSA instead optimizes the sparse networks directly at training time. Therefore, it has precise control over their creation process. This includes, for example, the computation of suitable batchnorm statistics, and the possibility of fine-

²In preliminary experiments we observed that using the SAM objective for ELSA leads to an increase of 1-2% accuracy in the ImageNet setting (dense and sparse). We do not include such experiments in this work, because they are orthogonal to our main contribution.

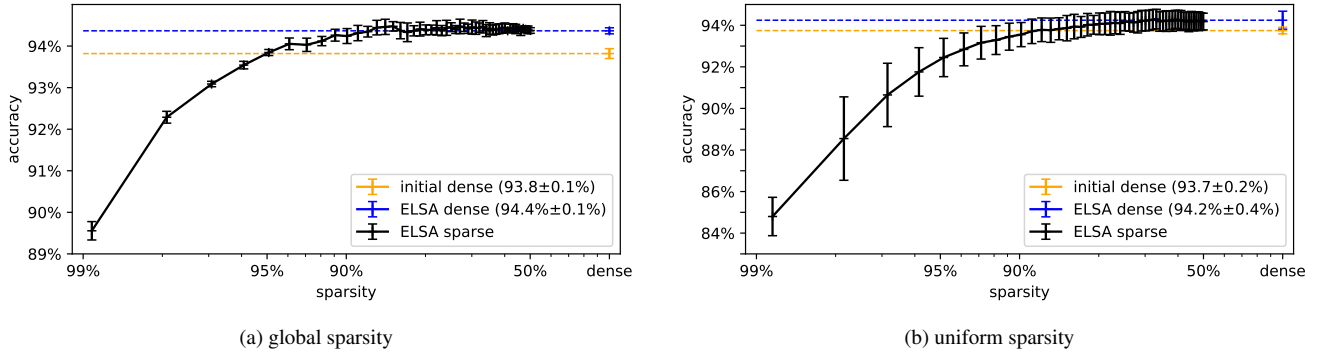


Figure 3. *Stress test experiments.* Multi-level ELSA is used to create 50 sparse models (CIFAR10, SpeedyResNet) embedded in a single dense one. x -axis: model sparsity (logarithmic in number of non-zero model parameters). y -axis: accuracy (mean and standard deviation). The dashed horizontal lines illustrate the accuracy of the initial dense network (orange) and the dense output of ELSA (blue), respectively.

tuning the sparse models before freezing and embedding them.

Alternating sparse and dense training steps One characteristic of ELSA is the alternation of sparsification and densification steps. Similar patterns have been proposed previously for other purposes.

DSD [14] trains a deep network by alternating between sparse phases, in which a sparsity pattern is fixed, and dense phases, in which all weights are allowed to change again. The goal, however, is not sparsification, but to increase the quality of the ultimate dense network. AC/DC [27] and GaP [23] follow similar patterns, but with the goal of producing sparse networks of highest possible accuracy.

The main difference of both methods to ELSA is that they do not preserve the sparse networks they produce during the process, but overwrite them. Instead of competitors to ELSA they are rather examples of an advanced densification (DSD) and sparsification (AC/DC, GaP) techniques that could be used as subroutines within ELSA.

Nested network structures Having groups of weights within a network that are learned at different times is a recurring pattern in the machine learning literature. Because of the space restrictions, we only highlight a few prominent examples here.

The classical *cascade correlation* architecture [8] learns the structure and weights of a (shallow) neural network by iteratively adding single neurons, learning their input weights, and then freezing those. In a continual learning scenario, *progressive networks* [32] extend previously trained network layers with additional neurons in order to continuously increase their capacity. Earlier parts of the network are frozen to prevent catastrophic forgetting. In the context of network sparsification, the *Lottery Ticket Hypothesis* [10] postulates that dense networks contain sparse subnetworks, which can be retrained from scratch to reach similar quality levels as the original network. FreezeNet [36]

freeze all weights except a small subset at their random value from initialization.

Most similar to our work is the *PackNet* framework [24]. It follows the same principle of sparsifying a network, freezing the non-zero weights and then training the remaining weights again. However, it does so in the context of continual multi-task learning, using different datasets for the different training phases. Network sparsification is used as a tool to free up capacity in the network, thereby allowing it to learn new tasks.

None of these methods share ELSA’s focus on easy storage and deployment of explicitly trained sparse models.

5. Conclusion

We have presented ELSA, a technique for constructing one or more sparse networks as embedded subsets of a single dense network. ELSA is completely flexible in the method used for sparsification and densification, in particular it puts no restriction on the loss function, the architecture, or the optimization technique. From the resulting ELSA-Nets fully trained networks of desired sparsity levels can be extracted effortlessly at prediction time. Thereby, ELSA vastly reduces the complexity of having to deploy different networks depending on the available resources, e.g., for mobile devices.

Our experiments showed that ELSA’s iterative way of producing sparse network results in networks of comparable quality to the gold standard of training sparse networks separately for each target sparsity level. The few discrepancies that we did observe provide us with promising future research directions. In cases where the ultimate dense network loses accuracy compared to its initial counterpart: is this an effect of the reduced network flexibility when some weights are frozen, or it is simply due to suboptimal choices of hyperparameters? In other cases, where the produced dense network was of higher accuracy than the initial one: is

this purely because it had undergone more training epochs? Or does the alternation of dense and sparse training steps together with the integration of frozen subset have also more fundamental consequences, for example on the loss landscape? We plan to study these questions in future work.

References

- [1] Myrtle.ai Blog. How to train your ResNet. <https://myrtle.ai/learn/how-to-train-your-resnet/>, . Accessed: 2023-10-15. 5, 6, 11
- [2] NeuralMagic Blog. Gradual magnitude pruning (GMP) hyperparameters. <https://neuralmagic.com/blog/gmp-hyperparameters/>, . Accessed: 2023-10-15. 5
- [3] Léon Bottou, Frank E Curtis, and Jorge Nocedal. Optimization methods for large-scale machine learning. *SIAM Review*, 60(2):223–311, 2018. 3
- [4] James Bradbury, Roy Frostig, Peter Hawkins, Matthew James Johnson, Chris Leary, Dougal Maclaurin, George Necula, Adam Paszke, Jake VanderPlas, Skye Wanderman-Milne, and Qiao Zhang. JAX: composable transformations of Python+NumPy programs, 2018. 5
- [5] Han Cai, Chuang Gan, Tianzhe Wang, Zhekai Zhang, and Song Han. Once-for-all: Train one network and specialize it for efficient deployment. In *International Conference on Learning Representations (ICLR)*, 2020. 7
- [6] Tianyi Chen, Bo Ji, Tianyu Ding, Biyi Fang, Guanyi Wang, Zhihui Zhu, Luming Liang, Yixin Shi, Sheng Yi, and Xiao Tu. Only train once: A one-shot neural network training and pruning framework. In *Conference on Neural Information Processing Systems (NeurIPS)*, 2021. 7
- [7] Jack Choquette, Wishwesh Gandhi, Olivier Giroux, Nick Stam, and Ronny Krashinsky. Nvidia a100 tensor core gpu: Performance and innovation. *IEEE Micro*, 41(2):29–35, 2021. 4, 5
- [8] Scott Fahlman and Christian Lebiere. The cascade-correlation learning architecture. In *Conference on Neural Information Processing Systems (NeurIPS)*, 1989. 8
- [9] Pierre Foret, Ariel Kleiner, Hossein Mobahi, and Behnam Neyshabur. Sharpness-aware minimization for efficiently improving generalization. In *International Conference on Learning Representations (ICLR)*, 2021. 7
- [10] Jonathan Frankle and Michael Carbin. The lottery ticket hypothesis: Finding sparse, trainable neural networks. In *International Conference on Learning Representations (ICLR)*, 2018. 8
- [11] Manas Gupta, Efe Camci, Vishandi Rudy Keneta, Abhishek Vaidyanathan, Ritwik Kanodia, Chuan-Sheng Foo, Min Wu, and Jie Lin. Is complexity required for neural network pruning? a case study on global magnitude pruning. *arXiv preprint arXiv:2209.14624*, 2022. 5
- [12] Masafumi Hagiwara. A simple and effective method for removal of hidden units and weights. *Neurocomputing*, 6(2): 207–218, 1994. 5
- [13] Song Han, Jeff Pool, John Tran, and William Dally. Learning both weights and connections for efficient neural network. In *Conference on Neural Information Processing Systems (NeurIPS)*, 2015. 4
- [14] Song Han, Jeff Pool, Sharan Narang, Huizi Mao, Enhao Gong, Shijian Tang, Erich Elsen, Peter Vajda, Manohar Paluri, John Tran, Bryan Catanzaro, and William J. Dally. DSD: Dense-sparse-dense training for deep neural networks. In *International Conference on Learning Representations (ICLR)*, 2016. 8
- [15] Jonathan Heek, Anselm Levskaya, Avital Oliver, Marvin Ritter, Bertrand Rondepierre, Andreas Steiner, and Marc van Zee. Flax: A neural network library and ecosystem for JAX, 2023. 5
- [16] John Hertz, Anders Krogh, and Richard G Palmer. *Introduction to the theory of neural computation*. Addison-Wesley Longman Publishing Co., Inc., 1991. 4
- [17] Torsten Hoeftler, Dan Alistarh, Tal Ben-Nun, Nikoli Dryden, and Alexandra Peste. Sparsity in deep learning: Pruning and growth for efficient inference and training in neural networks. *Journal of Machine Learning Research (JMLR)*, 2021. 5
- [18] E.D. Karnin. A simple procedure for pruning back-propagation trained neural networks. *IEEE Transactions on Neural Networks*, 1(2):239–242, 1990. 4
- [19] Diederik P Kingma and Jimmy Ba. Adam: A method for stochastic optimization. *International Conference on Learning Representations (ICLR)*, 2015. 3
- [20] Jungmin Kwon, Jeongseop Kim, Hyunseo Park, and In Kwon Choi. ASAM: Adaptive sharpness-aware minimization for scale-invariant learning of deep neural networks. In *International Conference on Machine Learning (ICML)*, 2021. 7
- [21] Joo Hyung Lee, Wonpyo Park, Nicole Mitchell, Jonathan Pilault, Johan S. Obando-Ceron, Han-Byul Kim, Namhoon Lee, Elias Frantar, Yun Long, Amir Yazdanbakhsh, Shivani Agrawal, Suvinay Subramanian, Xin Wang, Sheng-Chun Kao, Xingyao Zhang, Trevor Gale, Aart J. C. Bik, Woohyun Han, Milen Ferev, Zhonglin Han, Hong-Seok Kim, Yann Dauphin, Karolina Dziugaite, Pablo Samuel Castro, and Utku Evci. JaxPruner: A concise library for sparsity research. *arXiv preprint arXiv:2304.14082*, 2023. 5
- [22] Zhuang Liu, Jianguo Li, Zhiqiang Shen, Gao Huang, Shoumeng Yan, and Changshui Zhang. Learning efficient convolutional networks through network slimming. In *International Conference on Computer Vision (ICCV)*, 2017. 4
- [23] Xiaolong Ma, Minghai Qin, Fei Sun, Zejiang Hou, Kun Yuan, Yi Xu, Yanzhi Wang, Yen-Kuang Chen, Rong Jin, and Yuan Xie. Effective model sparsification by scheduled grow-and-prune methods. In *International Conference on Learning Representations (ICLR)*, 2022. 8
- [24] Arun Mallya and Svetlana Lazebnik. PackNet: Adding multiple tasks to a single network by iterative pruning. In *Conference on Computer Vision and Pattern Recognition (CVPR)*, 2018. 2, 8
- [25] Lu Miao, Xiaolong Luo, Tianlong Chen, Wuyang Chen, Dong Liu, and Zhangyang Wang. Learning pruning-friendly networks via Frank-Wolfe: One-shot, any-sparsity, and no retraining. In *International Conference on Learning Representations (ICLR)*, 2022. 7
- [26] Adam Paszke, Sam Gross, Francisco Massa, Adam Lerer, James Bradbury, Gregory Chanan, Trevor Killeen, Zem

- ing Lin, Natalia Gimelshein, Luca Antiga, Alban Desmaison, Andreas Kopf, Edward Yang, Zachary DeVito, Martin Raison, Alykhan Tejani, Sasank Chilamkurthy, Benoit Steiner, Lu Fang, Junjie Bai, and Soumith Chintala. PyTorch: An imperative style, high-performance deep learning library. In *Conference on Neural Information Processing Systems (NeurIPS)*. 2019. 5
- [27] Alexandra Peste, Eugenia Iofinova, Adrian Vladu, and Dan Alistarh. AC/DC: Alternating Compressed/DeCompressed Training of Deep Neural Networks. In *Conference on Neural Information Processing Systems (NeurIPS)*, 2021. 5, 8
- [28] Alexandra Peste, Adrian Vladu, Eldar Kurtic, Christoph H. Lampert, and Dan Alistarh. CrAM: A compression-aware minimizer. In *International Conference on Learning Representations (ICLR)*, 2023. 7
- [29] Russell Reed. Pruning algorithms-a survey. *IEEE Transactions of Neural Networks (TNN)*, 4(5):740–747, 1993. 4
- [30] Herbert Robbins and Sutton Monro. A Stochastic Approximation Method. *The Annals of Mathematical Statistics*, 22(3):400 – 407, 1951. 3
- [31] Sebastian Ruder. An overview of gradient descent optimization algorithms. *arXiv preprint arXiv:1609.04747*, 2016. 3
- [32] Andrei A Rusu, Neil C Rabinowitz, Guillaume Desjardins, Hubert Soyer, James Kirkpatrick, Koray Kavukcuoglu, Razvan Pascanu, and Raia Hadsell. Progressive neural networks. *arXiv preprint arXiv:1606.04671*, 2016. 8
- [33] Derya Soydaner. A comparison of optimization algorithms for deep learning. *International Journal of Pattern Recognition and Artificial Intelligence*, 34(13), 2020. 3
- [34] Shivangi Srivastava, Maxim Berman, Matthew B. Blaschko, and Devis Tuia. Adaptive compression-based lifelong learning. In *British Machine Vision Conference (BMVC)*, 2019. 2
- [35] Ross Wightman, Hugo Touvron, and Hervé Jégou. ResNet strikes back: An improved training procedure in timm. *arXiv preprint arXiv:2110.00476*, 2021. 5
- [36] Paul Wimmer, Jens Mehnert, and Alexandru Condurache. Freezenet: Full performance by reduced storage costs. In *Asian Conference on Computer Vision (ACCV)*, 2020. 8
- [37] Sergey Zagoruyko and Nikos Komodakis. Wide residual networks. In *British Machine Vision Conference (BMVC)*, 2016. 5
- [38] Yuxin Zhang, Mingbao Lin, Zhihang Lin, Yiting Luo, Ke Li, Fei Chao, Yongjian Wu, and Rongrong Ji. Learning best combination for efficient N:M sparsity. In *Conference on Neural Information Processing Systems (NeurIPS)*, 2022. 4
- [39] Max Zimmer, Christoph Spiegel, and Sebastian Pokutta. Compression-aware training of neural networks using Frank-Wolfe. *arXiv preprint arXiv:2205.11921*, 2022. 7

A. Appendix – Experimental Details

Our experiments use standard benchmarks from the network pruning literature. For details of the implementation, see the attached source code.

A.1. ImageNet

Dataset The *ImageNet2012* dataset consists of 1.2 million training examples, which we use for training and model selection, and 50,000 validation examples, which we use for the final model evaluation. Images have variable sizes.

We use the standard preprocess pipeline of the flax neural network library. For training, the input images are decoded and a patch is extracted using tensorflow’s `tf.image.sample_distorted_bounding_box` function. These are scaled to 224×224 resolution and with 50% probability flipped horizontally. For evaluation, a center patch is extracted from the decoded images and scaled to 224×224 with no further augmentation steps. In both cases, the resulting image values are then normalized by subtracting the mean and dividing by the standard deviation.

Model For ImageNet, use a standard ResNet50 as provided in the flax neural network library. It has 25,610,152 parameters, out of which 53,120 (0.2%) are the batchnorm statistics. This network is known to allow high accuracy, even when trained from scratch, at reasonable training and inference cost. In line with prior work, we sparsify it to 90%, 80% and 70% zero weights for unstructured sparsity (global or uniform). For semi-structured sparsity we use 1 : 8(87.5%), 1 : 4(75%) and 2 : 4(50%).

A.2. CIFAR

Datasets The *CIFAR10* and *CIFAR100* datasets each consists of 60,000 training examples, which we use for training and model selection, and 10,000 test examples, which we

use for the finale model evaluation. All images are of size 32×32 .

For training, the images are padded by 4 pixels on each side, and then a 32×32 patch is extracted from a random position. These are flipped horizontally with 50% probability. The resulting images are then normalized as above. For evaluation, no preprocessing is applied except for the normalization.

Models For CIFAR100, we use a standard WideResNet-28-10 with 36,554,836 parameters, out of which 17,952 (0.05%) are the batchnorm statistics. This architecture is known to achieve state-of-the-art accuracy among ConvNets at modest compute requirements. It is highly over-parametrized, though, such that high sparsification ratios are possible. In our experiments, we use 95%, 90% and 80% for unstructured sparsity. Lower sparsity values tend not to lead to higher accuracy for this setting. For semi-structured sparsity we use the same patterns as above.

For CIFAR10, we use a *SpeedyResNet* architecture as described in [1]. It has 4,658,140 parameters out of which 3,584 (0.08%) are the batchnorm statistics. This small architecture is designed particularly for high efficiency at training and inference time. In our implementation one training epoch takes approximately 3 seconds on a A100 GPU, and a complete training run of 30 epochs less than 2 minutes. That allows us to perform experiments in many different settings, including 50 different sparsity levels (99%, ..., 50%).

parameter	CIFAR10 (SpeedyResNet)	CIFAR100 (WideResNet-28-10)	ImageNet (ResNet50)
batch size	512	256	1024
learning rate	$0.2 \cdot \frac{\text{batchsize}}{256}$	$0.1 \cdot \frac{\text{batchsize}}{256}$	$0.1 \cdot \frac{\text{batchsize}}{256}$
number of epochs	30	100	100
number of warmup epochs	3	3	5
optimizer	SGD	SGD	SGD
momentum	0.9	0.9	0.9
Nesterov acceleration	yes	yes	yes
dropout rate	—	—	0.3
weight-decay	0.0005	0.0005	0.0001
label smoothing	0.1	0.1	0.1
floating point type	float32	bfloat16	bfloat16

Table 5. Training Hyperparameter